Distributed Bipartite-Scaled Consensus Control of Leader-Follower MASs under Directed Fixed/Switching Topologies

Siyu Liu, Jie Zhang, Junping Wang, and Dawei Ding

Abstract—**This paper investigates bipartite-scaled consensus for leader-follower linear multi-agent systems (MASs) under directed fixed or switching cooperative-competitive topologies. The followers are partitioned into two subgroups with cooperative interactions within each subgroup and competitive interactions across subgroups. Prescribed scaling factors are introduced to achieve specified proportional relationships, thereby relaxing the conventional bipartite consensus condition that forces the two subgroups to converge to equal magnitude but opposite sign. This feature is particularly beneficial for complex systems where different subgroups require distinct influence levels from the leader. When full state information is available, a distributed state feedback controller is developed and consensus conditions are derived via algebraic graph theory and Lyapunov stability theory. For scenarios where states are not directly measurable, an observer-based output feedback controller is constructed and the closed-loop stability is rigorously analyzed. Furthermore, both strategies are extended to switching topologies with corresponding sufficient conditions established. Numerical simulations validate the theoretical findings.**

Index Terms—**Bipartite-scaled consensus, leader-follower multi-agent systems (MASs), fixed/switching topologies, output feedback**

I. Introduction

MULTI-agent systems (MASs) have attracted significant attention due to their broad applications in unmanned systems [1], smart grids [2], and connected vehicles [3]. Consensus aims to asymptotically drive the states of all agents to a common value via distributed protocols [4–6]. Among various consensus settings, the leader-follower framework is particularly important, because it enables a designated leader agent to steer the behavior of the whole group, which is essential in many complex systems where a reference trajectory or command must be tracked.

Traditional consensus control typically relies on cooperative interactions among agents and achieves state synchronization under nonnegative graphs. However, in practical scenarios with antagonistic relationships, such as social networks and distributed decision-making systems, conventional strategies cannot be directly applied. For instance, in cooperative combat of multiple unmanned aerial vehicles, different formations may need to execute opposite tasks [7]. To address this issue, signed graphs have been introduced to capture competitive interactions, leading to the notion of bipartite consensus, where the two subgroups converge to values with equal magnitude and opposite sign [8]. Along this line, various results have been reported. For second-order MASs, finite-time and fixed-time bipartite consensus tracking is studied using integral sliding-mode control in Ref. [9]. For leaderless high-order linear systems, a novel in-degree balanced condition is proposed to achieve group-bipartite consensus under cooperative and antagonistic interactions in Ref. [10]. For nonlinear disturbed systems, event-triggered fixed-time bipartite consensus is studied in Ref. [11]. Despite these advances, bipartite consensus imposes a rigid constraint: the two subgroups must converge to exactly symmetric values. In many complex systems, different subgroups may need to follow the leader with different relationships, rather than a fixed opposite pattern. This limitation naturally motivates the exploration of a more flexible consensus mechanism.

Different from classical consensus, scaled consensus introduces scaling factors to achieve flexible convergence among multiple subgroups, driving agents toward prespecified ratios instead of a common value. This concept is especially useful in heterogeneous robot formations where different types of robots must maintain specific relative positions. Early studies on scaled consensus primarily focused on the first-order integrator agents. Reference [12] obtains the necessary and sufficient criteria for scaled consensus in the presence of output saturation via an integral Lyapunov function. Reference [13] addresses the impact of Markovian switching topologies and communication noises on the first-order MASs by adopting time-varying gains to suppress noise and deriving sufficient conditions for mean square scaled consensus. For the switched first-order systems consisting of continuous-time and discrete-time subsystems, scaled consensus with asymptotic, finite-time, and fixed-time convergence rates is analyzed in Ref. [14]. Beyond the first-order settings, higher-order MASs have also been considered. In Ref. [15], a dynamic event-triggered scaled consensus scheme is developed for reliable and unreliable networks, with a resilient mechanism further proposed to

Manuscript received: 30 April 2026; revised: 20 May 2026; accepted: 27 May 2026. *(Corresponding author: Jie Zhang.)*

Citation: S. Liu, J. Zhang, J. Wang, and D. Ding, Distributed bipartite-scaled consensus control of leader-follower MASs under directed fixed/switching topologies, *Int. J. Intell. Control Syst.*, 2026, 31(2), 173–184.

Siyu Liu, Jie Zhang, and Junping Wang are with School of Electronics Information Engineering, Taiyuan University of Science and Technology, Taiyuan 030024, China (e-mail: siyu_liu_2003@163.com; zhangjie_hao666@163.com; wangjun3274@163.com).

Dawei Ding is with School of Automation and Electrical Engineering, University of Science and Technology Beijing, Beijing 100083, China (e-mail: dingdawei@ustb.edu.cn).

Digital Object Identifier 10.62678/IJICS202606.10367

counteract denial-of-service attacks. More recently, event-triggered proportional consensus with input constraints in adversarial networks is investigated in Ref. [16]. However, none of the above works incorporate a leader-follower framework where the scaling factors between subgroups and the leader can be freely assigned. In the most existing results on scaled consensus, the scaling relationship is either fixed or not explicitly linked to a leader agent. This gap naturally motivates the study of bipartite-scaled consensus in a leader-follower setting with prescribed scaling factors.

Nevertheless, the aforementioned works mainly focus on either bipartite or scaled consensus for single-task scenarios. Research on composite group consensus for more complex tasks remains limited. In bipartite scaled consensus, a more challenging scenario arises: agents are divided into two antagonistic subgroups and each subgroup converges to scaled versions of a reference signal with opposite signs. Consider a multi-robot reconnaissance mission, one subgroup follows the leader's trajectory in the same direction at a lower speed ratio, while the other moves opposite at a higher ratio. Conventional bipartite consensus cannot realize such differentiated scaling. The proposed method directly addresses this by allowing free assignment of scaling factors to each follower. This composite objective cannot be captured by pure bipartite or pure scaled consensus alone. Although bipartite scaled consensus has been explored, existing results apply only to leaderless systems. In many practical complex MASs, a leader agent is essential to steer the group, making the leader-follower setting more relevant. Thus, bipartite-scaled consensus in the leader-follower framework remains an open problem.

Moreover, most existing studies assume that the communication topology is fixed. In practical applications, communication link failures, signal attenuation, and network reconfiguration often lead to time-varying structures. Switching topologies provide a more accurate description of such dynamic scenarios and have thus become an important direction in cooperative control of MASs [17]. Several recent efforts have addressed consensus under switching topologies. Specifically, Ref. [18] solves the bipartite leaderless position consensus problem for heterogeneous uncertain MASs with directed switching topologies, and Ref. [19] studies scaled consensus for heterogeneous MASs under switching topologies using a predictive controller to compensate for communication delays. However, these works do not simultaneously address the coexistence of cooperative-competitive interactions, flexible scaling ratios, dynamic topology switching, and a leader-follower framework. The coupling of these factors introduces significant challenges: the control design must accommodate antagonistic behaviors, time-varying communication structures, and prescribed scaling ratios concurrently. Up to now, research on such composite group consensus problems remains scarce. Motivated by this gap, this paper investigates bipartite-scaled consensus for leader-follower MASs under both fixed and switching topologies, with the primary contributions summarized as follows:

(1) A new framework for bipartite-scaled consensus in leader-follower MASs is established. Unlike conventional bipartite consensus that enforces symmetric convergence with opposite signs, flexible scaling factors assignable to each subgroup are introduced. Leveraging signed graph theory and the M-matrix property, a gauge transformation converts the bipartite tracking problem into a standard consensus problem, enabling stability analysis without eigenvalue symmetry.

(2) Both distributed state feedback and observer-based output feedback controllers are designed. For unmeasurable states, an observer is constructed using the detectable condition and a linear matrix inequality (LMI). The separation principle for signed directed graphs is established, allowing independent design of the feedback and observer gains while accommodating prescribed scaling factors and preserving closed-loop stability under cooperative-competitive interactions.

(3) The protocols are extended to switching topologies. A common Lyapunov function method guarantees exponential consensus under arbitrary non-Zeno switching signals without any dwell-time condition. The results unify purely cooperative scaled consensus, standard bipartite consensus, and the proposed bipartite-scaled consensus within a general non-negative graph framework.

All notations adopted in this work are summarized in Table 1 for reference.

Table 1 Notations.

Symbol	Meaning
$\mathbb{R}$	Set of real numbers
$\mathbb{R}^n$	n-dimensional real vector space
$\mathbb{R}^{n\times m}$	Set of $n\times m$ real matrices
$\mathrm{sgn}(\cdot)$	Sign function
$\mathrm{diag}(A_1,A_2,\ldots,A_N)$	Block diagonal matrix with blocks $A_1,A_2,\ldots,A_N$
$\otimes$	Kronecker product
I_N	N-dimensional identity matrix
1_N	All-one column vector in $\mathbb{R}^N$
$\lambda_i(A)$	The i-th eigenvalue of matrix A
$\lambda_{\max}(\cdot)$ and $\lambda_{\min}(\cdot)$	Maximum and minimum eigenvalues
$\mathrm{Re}(z)$	Real part of complex number z

II. Preliminaries

A. Graph Theory

To describe the cooperative and antagonistic interactions among multiple agents, a directed signed graph $\mathcal{G}(\mathcal{V},\mathcal{E},\mathcal{A})$ is introduced, where $\mathcal{V}=\{0,1,\ldots,N\}$ denotes the node set consisting of N followers and one leader, $\mathcal{E}\subseteq\{(i,j)\mid i,j\in\mathcal{V}, i\neq j\}$ represents the edge set, and $\mathcal{A}=[a_{ij}]$ is the signed adjacency matrix. An edge $(j,i)\in\mathcal{E}$ indicates that node i can receive information from node j. The sign of a_{ij} reflects the nature of the interaction: $a_{ij}>0$ denotes cooperative interaction, while $a_{ij}<0$ denotes antagonistic interaction. In particular, $a_{ij}=0$, if no edge exists from node j to node i. The neighbor set of node i is defined as $\mathcal{N}_i=\{j\in\mathcal{V}\mid(i,j)\in\mathcal{E}\}$. The Laplacian matrix $L=[l_{ij}]$ associated with $\mathcal{G}$ is defined as $l_{ii}=\sum_{j=1}^{N}a_{ij}$ and $l_{ij}=-a_{ij}$ for $i\neq j$.

A directed signed graph $\mathcal{G}$ is said to be structurally balanced if the node set $\mathcal{V}$ can be partitioned into two nonempty subsets $\mathcal{V}_1$ and $\mathcal{V}_2$ such that $a_{ij} \geqslant 0$ for any $i, j \in \mathcal{V}_p$, $p = 1,2$ and $a_{ij} \leqslant 0$ for any $i \in \mathcal{V}_p$ and $j \in \mathcal{V}_q$ with $q = 3-p$. Under this condition, there is a diagonal signature matrix $\mathcal{D} = \mathrm{diag}(d_1, d_2, \ldots, d_N)$ with $d_i \in \{-1,1\}$. The leader node is labeled as node 0 and the pinning matrix is defined as $G = \mathrm{diag}(g_1, g_2, \ldots, g_N)$, where $g_i > 0$ if follower i has direct access to the leader's information and $g_i = 0$ otherwise. The graph $\mathcal{G}$ in this paper is directed and contains a spanning tree rooted at the leader, ensuring the connectivity of the overall system. Then we have Lemma 1.

Lemma 1 [20] If the directed graph $\mathcal{G}$ is structurally balanced, there is a diagonal signature matrix $\mathcal{D}$ such that $\bar{L} = \mathcal{D}(L+G)\mathcal{D}$ is positive definite if the directed spanning tree condition is satisfied.

Remark 1 The matrix $\bar{L}$ is generally nonsymmetric, yet it remains an M-matrix with a positive definite symmetric part from Lemma 1. Consequently, there is a positive diagonal matrix Π such that

$$\Pi \bar{L} + \bar{L}^{\mathrm{T}} \Pi > 0 \tag{1}$$

This property, known as diagonal stability, overcomes the difficulty caused by asymmetry and enables stability analysis without imposing real eigenvalue assumptions. The existence of such Π follows from standard results on M-matrices under the spanning tree condition.

B. Problem Formulation

Consider an MAS consisting of a group of agents. The communication topology among agents is described by a directed signed graph. The dynamics of each follower can be given as

$$\begin{cases} \dot{x}_i(t) = Ax_i(t) + Bu_i(t), \\ y_i(t) = Cx_i(t) + Du_i(t), \end{cases} \quad i = 1, 2, \ldots, N \tag{2}$$

where $x_i(t) \in \mathbb{R}^n$, $u_i(t) \in \mathbb{R}^m$, and $y_i(t) \in \mathbb{R}^p$ denote the state vector, control input vector, and output vector of the i-th follower. A, B, C, and D denote the system matrices with appropriate dimensions, respectively.

The leader, which generates the reference trajectory, is described as

$$\begin{cases} \dot{x}_0(t) = Ax_0(t), \\ y_0(t) = Cx_0(t) \end{cases} \tag{3}$$

where $x_0(t) \in \mathbb{R}^n$ and $y_0(t) \in \mathbb{R}^p$ are the state vector and output vector of the leader.

For the system matrices of followers and leader, Assumption 1 needs to be satisfied.

Assumption 1 The matrix pair (A, B) is stabilizable and the matrix pair (A, C) is detectable.

The bipartite-scaled tracking error of each agent is defined as

$$\delta_i(t) = \frac{x_i(t)}{\omega_i} - d_i \frac{x_0(t)}{\omega_0}, \quad i = 1, 2, \ldots, N \tag{4}$$

where $\omega_i > 0$ is prescribed scaling factor, and denotes the bipartite-scaled tracking error of the i-th follower based on the actual state. Collectively, they form the diagonal matrix $\Omega = \mathrm{diag}(\omega_1, \omega_2, \ldots, \omega_N)$, whose entries can be arbitrarily assigned to each follower. Here d_i is the i-th diagonal element of the signature matrix $\mathcal{D} = \mathrm{diag}(d_1, d_2, \ldots, d_N)$, with $d_i \in \{-1,1\}$ indicating the subgroup membership of follower i ($d_i = 1$ for $\mathcal{V}_1$ and $d_i = -1$ for $\mathcal{V}_2$). The scaling factors ω_i allow each follower to converge to a user-specified proportion of the leader's scaled state, rather than a fixed common value.

Problem 1 Given the MAS described by Eqs. (2) and (3) under a structurally balanced directed graph $\mathcal{G}$ and design a distributed state feedback controller such that the following asymptotic bipartite-scaled consensus is achieved.

$$\begin{cases} \lim\limits_{t\to\infty} \left(\dfrac{x_i(t)}{\omega_i} - d_i \dfrac{x_0(t)}{\omega_0} \right) = 0, \\ \lim\limits_{t\to\infty} \left(\dfrac{x_i(t)}{\omega_i} + d_i \dfrac{x_0(t)}{\omega_0} \right) = 0 \end{cases} \tag{5}$$

Remark 2 Equation (5) indicates that the scaled states of followers in the two subgroups converge to the leader's scaled state with opposite signs. The main novelty lies in the scaling factor ω_i, which can be freely assigned to each follower. This relaxes the rigid constraint of conventional bipartite consensus, where the two subgroups are forced to converge to values of equal magnitude and opposite sign. In our framework, different subgroups or even individual followers can track the leader with distinct prescribed proportions, enabling flexible coordination in complex systems where subgroups require different influence levels from the leader. Moreover, under the assumptions of structural balance and a spanning tree rooted at the leader, the bipartite-scaled consensus problem can be transformed into a standard consensus problem via a gauge transformation, which facilitates the design of distributed controllers for fixed and switching topologies as well as observer-based output feedback.

III. MAIN RESULTS

This section investigates the bipartite-scaled consensus problem for MASs described by Eqs. (2) and (3) under both fixed and switching topologies. The state feedback controller is first designed assuming full state availability under fixed topologies, and then extended to switching topologies. Subsequently, an observer-based controller is proposed for the case where only output measurements are accessible and its performance under switching topologies is also analyzed. Detailed designs and convergence analyses are presented in the following subsections.

A. Bipartite-Scaled Consensus via State Feedback under Fixed Topologies

To facilitate the distributed control design, the neighborhood consensus error for each follower is defined as

$$\begin{aligned} \varepsilon_i(t) = &\sum_{j \in N_i} |a_{ij}| \left(\frac{x_i(t)}{\omega_i} - \mathrm{sgn}(a_{ij}) \frac{x_j(t)}{\omega_j} \right) + \\ &g_i \left(\frac{x_i(t)}{\omega_i} - d_i \frac{x_0(t)}{\omega_0} \right) \end{aligned} \tag{6}$$

where the first term captures the relative scaled states between neighboring followers and the second term introduces pinning to the leader.

Based on Eq. (6), a distributed state feedback controller is proposed as

$$u_i(t) = c\Gamma\varepsilon_i(t) \tag{7}$$

where $c < 0$ and $\Gamma \in \mathbb{R}^{m\times n}$ are the coupling strength and the feedback gain, respectively.

Define the global stacked vectors

$$\begin{aligned}&\varepsilon(t) = (\varepsilon_1^{\mathrm{T}}(t), \varepsilon_2^{\mathrm{T}}(t), \ldots, \varepsilon_N^{\mathrm{T}}(t))^{\mathrm{T}},\\ &x(t) = (x_1^{\mathrm{T}}(t), x_2^{\mathrm{T}}(t), \ldots, x_N^{\mathrm{T}}(t))^{\mathrm{T}},\\ &\bar{x}_0(t) = 1_N \otimes x_0(t)\end{aligned} \tag{8}$$

Substituting Eq. (6) into the global dynamics yields

$$\begin{aligned}\dot{x}(t) = {}&(I_N \otimes A)x(t) + (I_N \otimes B)u(t) =\\ &(I_N \otimes A)x(t) + c(I_N \otimes B\Gamma)\varepsilon(t) =\\ &(I_N \otimes A + c(L+G)\Omega^{-1} \otimes B\Gamma)x(t) -\\ &c(G\mathcal{D}\Omega_0^{-1} \otimes B\Gamma)\bar{x}_0(t)\end{aligned} \tag{9}$$

where $\Omega = \mathrm{diag}(\omega_1, \omega_2, \ldots, \omega_N)$ is the diagonal matrix of scaling factors and $\mathcal{D} = \mathrm{diag}(d_1, d_2, \ldots, d_N)$ is the signature matrix. The scalar $\omega_0 > 0$ is the leader's scaling factor. Equation (9) can be written compactly as

$$\dot{x}(t) = A_c x(t) + B_c \bar{x}_0(t) \tag{10}$$

with

$$\begin{aligned}&A_c = I_N \otimes A + c(L+G)\Omega^{-1} \otimes B\Gamma,\\ &B_c = -c(G\mathcal{D}\omega_0^{-1} \otimes B\Gamma)\end{aligned} \tag{11}$$

Due to the coexistence of cooperative and antagonistic interactions in the directed signed graph, the following equivalence relations can be established for any pair of agents.

$$\begin{cases}|a_{ij}| = a_{ij}\mathrm{sgn}(a_{ij}),\\ a_{ij}d_i = |a_{ij}|d_j,\\ |a_{ij}|d_i = a_{ij}d_i\mathrm{sgn}(a_{ij}) = |a_{ij}|d_j\mathrm{sgn}(a_{ij})\end{cases} \tag{12}$$

These relations play a crucial role in transforming the bipartite consensus problem into a conventional consensus problem, as will be shown in the subsequent analysis.

According to Eq. (4), we have

$$\begin{aligned}\dot{\delta}_i(t) = {}&\frac{\dot{x}_i(t)}{\omega_i} - d_i\frac{\dot{x}_0(t)}{\omega_0} =\\ &\omega_i^{-1}Ax_i(t) + c\omega_i^{-1}B\Gamma\sum_{j\in N_i}|a_{ij}|\frac{x_i(t)}{\omega_i} -\\ &\omega_i^{-1}B\Gamma\sum_{j\in N_i}|a_{ij}|\left(\mathrm{sgn}(a_{ij})\frac{x_j(t)}{\omega_j}\right) +\\ &c\omega_i^{-1}B\Gamma g_i\left(\frac{x_i(t)}{\omega_i} - d_i\frac{x_0(t)}{\omega_0}\right) - d_i\frac{Ax_0(t)}{\omega_0}\end{aligned} \tag{13}$$

Substituting $\dfrac{x_i(t)}{\omega_i} = \delta_i(t) + d_i\dfrac{x_0(t)}{\omega_0}$ into Eq. (9), we obtain

$$\begin{aligned}\dot{\delta}_i(t) = {}&A\delta_i(t) +\\ &c\omega_i^{-1}B\Gamma\sum_{j\in N_i}|a_{ij}|(\delta_i(t) - \mathrm{sgn}(a_{ij})\delta_j(t)) +\\ &c\omega_i^{-1}B\Gamma\sum_{j\in N_i}|a_{ij}|g_i\delta_i(t)\end{aligned} \tag{14}$$

Based on the above derivations, the global consensus error dynamics can be expressed as

$$\dot{\delta}(t) = (I_N \otimes A + c(L+G)\Omega^{-1} \otimes B\Gamma)\delta(t) \tag{15}$$

That is

$$\dot{\delta}(t) = A_c\delta(t) \tag{16}$$

where A_c is defined in Eq. (11). This linear time-invariant system characterizes the evolution of the bipartite tracking error for all followers.

To analyze the stability of the error system in Eq. (16), a nonsingular transformation is introduced to simplify the proof. Define the transformed vector as

$$\bar{\delta}(t) = (\mathcal{D} \otimes I_n)\delta(t) \tag{17}$$

Since $\mathcal{D}\mathcal{D} = I_N$, the dynamics of $\bar{\delta}(t)$ can be derived as

$$\begin{aligned}\dot{\bar{\delta}}(t) = {}&(\mathcal{D}\otimes I_n)\dot{\delta}(t)(\mathcal{D}\otimes I_n)(I_N\otimes A)(\mathcal{D}\otimes I_n)\bar{\delta}(t) +\\ &c(\mathcal{D}\otimes I_n)((L+G)\Omega^{-1}\otimes B\Gamma)(\mathcal{D}\otimes I_n)\bar{\delta}(t) =\\ &(I_N \otimes A + c\mathcal{D}(L+G)\mathcal{D}\Omega^{-1} \otimes B\Gamma)\bar{\delta}(t)\end{aligned} \tag{18}$$

Recall from Lemma 1 that $\bar{L} = \mathcal{D}L_s\mathcal{D}$. Under the spanning tree condition, $\bar{L}$ is positive definite. Then the transformed error dynamics can be rewritten as

$$\dot{\bar{\delta}}(t) = (I_N \otimes A + c\bar{L}\Omega^{-1} \otimes B\Gamma)\bar{\delta}(t) \tag{19}$$

Compared with the original error system in Eq. (16), the transformed system in Eq. (19) has a more tractable structure, where the matrix $\bar{L}$ is positive definite and the bipartite nature of the problem has been absorbed into the transformation. Lemma 2 provides a key stability condition.

Lemma 2 If the matrix pair (A, B) is stabilizable, for any $\alpha \geqslant 0$ there are a positive definite matrix $P = P^{\mathrm{T}} > 0$ and a scalar $\tau > 0$ such that the inequality holds true

$$AP + PA^{\mathrm{T}} - \tau BB^{\mathrm{T}} + \alpha P < 0 \tag{20}$$

Proof Since (A, B) is stabilizable, there is a feedback gain F such that $A+BF$ is Hurwitz, i.e., all eigenvalues of $A+BF$ have negative real parts. Let $\eta = \max\mathrm{Re}(\lambda(A+BF)) < 0$ and define $\alpha_0 = -\eta > 0$. Then, for any α satisfying $0 \leqslant \alpha < \alpha_0$, the Lyapunov stability theorem guarantees the existence of a positive definite matrix $P = P^{\mathrm{T}} > 0$ such that

$$(A+BF)P + P(A+BF)^{\mathrm{T}} + \alpha P < 0 \tag{21}$$

Set $K = FP$ and expand the left-hand side of Formula (21) to obtain

$$AP + PA^{\mathrm{T}} + BK + K^{\mathrm{T}}B^{\mathrm{T}} + \alpha P < 0 \tag{22}$$

Note that the term $BK + K^{\mathrm{T}}B^{\mathrm{T}}$ is indefinite. By the projection lemma in Ref. [21], the scalar $\tau > 0$ exists satisfying the inequality below.

$$AP + PA^{\mathrm{T}} - \tau BB^{\mathrm{T}} + \alpha P < 0 \tag{23}$$

This completes the proof. ■

The main theorem under the proposed state feedback controller in Eq. (7) is stated as follows.

Theorem 1 For the leader-follower MAS governed by Eqs. (2) and (3) over a structurally balanced directed graph with a spanning tree rooted at the leader, bipartite-scaled consensus can be realized via the distributed state feedback controller in Eq. (7) under Assumption 1 for any given positive scaling factor $\omega_i > 0$, provided that the subsequent conditions are satisfied.

(1) The coupling strength satisfies $c < 0$.

(2) The feedback gain matrix is designed as $\Gamma = B^{\mathrm{T}}P_1$, where $P_1 = P_1^{\mathrm{T}} > 0$ is a matrix solution of Formula (20) in Lemma 2.

Proof From Remark 1, there is a positive diagonal matrix Π such that $\Pi\bar{L}+\bar{L}^{\mathrm{T}}\Pi > 0$. Since $\bar{L}$ is an M-matrix and Ω^{-1} is positive diagonal, one may directly take $\Pi = \Omega^{-1}$. This choice satisfies the inequality because $\Omega^{-1}\bar{L}+\bar{L}^{\mathrm{T}}\Omega^{-1} = \Omega^{-1}(\bar{L}+\bar{L}^{\mathrm{T}})\Omega^{-1} > 0$. The right-hand side is positive definite since $\bar{L}+\bar{L}^{\mathrm{T}} > 0$ and $\Omega^{-1} > 0$.

Define the symmetric matrix

$$\Lambda = \frac{1}{2}(\Pi\bar{L}\Omega^{-1}+\Omega^{-1}\bar{L}^{\mathrm{T}}\Pi) \tag{24}$$

with $\Pi = \Omega^{-1}$ and $\Lambda = \Omega^{-1}(\bar{L}+\bar{L}^{\mathrm{T}})\Omega^{-1}/2$, which is clearly positive definite. Let $\mu = \lambda_{\min}(\Lambda) > 0$.

To analyze the stability of the transformed error system in Eq. (19), we construct the following Lyapunov function.

$$V(t) = \bar{\delta}(t)^{\mathrm{T}}(\Pi\otimes P_1)\bar{\delta}(t) \tag{25}$$

where $P_1 = P_1^{\mathrm{T}} > 0$ satisfies Lemma 2 and the feedback gain is chosen as $\Gamma = B^{\mathrm{T}}P_1$.

Differentiating $V(t)$ along the trajectory of Eq. (19) yields

$$\begin{aligned}\dot{V}(t) = \dot{\bar{\delta}}(t)^{\mathrm{T}}(\Pi\otimes P_1)\bar{\delta}(t)+\bar{\delta}(t)^{\mathrm{T}}(\Pi\otimes P_1)\dot{\bar{\delta}}(t) = \\ \bar{\delta}(t)^{\mathrm{T}}(\Pi\otimes(A^{\mathrm{T}}P_1+P_1A))\bar{\delta}(t)+ \\ c\bar{\delta}(t)^{\mathrm{T}}((\bar{L}\Omega^{-1})^{\mathrm{T}}\Pi\otimes(B\Gamma)^{\mathrm{T}}P_1+ \\ \Pi\bar{L}\Omega^{-1}\otimes P_1B\Gamma)\bar{\delta}(t)\end{aligned} \tag{26}$$

Substituting $\Gamma = B^{\mathrm{T}}P_1$ into Eq. (26) gives

$$\begin{aligned}\dot{V}(t) = \bar{\delta}(t)^{\mathrm{T}}(\Pi\otimes(A^{\mathrm{T}}P_1+P_1A))\bar{\delta}(t)+ \\ c\bar{\delta}(t)^{\mathrm{T}}((\bar{L}\Omega^{-1})^{\mathrm{T}}\Pi\otimes P_1BB^{\mathrm{T}}P_1+ \\ \Pi\bar{L}\Omega^{-1}\otimes P_1BB^{\mathrm{T}}P_1)\bar{\delta}(t)\end{aligned} \tag{27}$$

Using the Kronecker product property, the two terms can combine as

$$\begin{aligned}(\bar{L}\Omega^{-1})^{\mathrm{T}}\Pi\otimes P_1BB^{\mathrm{T}}P_1+\Pi\bar{L}\Omega^{-1}\otimes P_1BB^{\mathrm{T}}P_1 = \\ ((\bar{L}\Omega^{-1})^{\mathrm{T}}\Pi+\Pi\bar{L}\Omega^{-1})\otimes P_1BB^{\mathrm{T}}P_1\end{aligned} \tag{28}$$

From the definition of Λ in Eq. (24), we can obtain

$$(\bar{L}\Omega^{-1})^{\mathrm{T}}\Pi+\Pi\bar{L}\Omega^{-1} = 2\Lambda \tag{29}$$

Thus Eq. (27) simplifies to

$$\begin{aligned}\dot{V}(t) = \bar{\delta}(t)^{\mathrm{T}}(\Pi\otimes(A^{\mathrm{T}}P_1+P_1A))\bar{\delta}(t)+ \\ 2c\bar{\delta}(t)^{\mathrm{T}}(\Lambda\otimes P_1BB^{\mathrm{T}}P_1)\bar{\delta}(t)\end{aligned} \tag{30}$$

Because $\Lambda \geqslant \mu I_N$ in the sense, $\Lambda-\mu I_N$ is positive semidefinite. Consequently, we have

$$\Lambda\otimes P_1BB^{\mathrm{T}}P_1 \geqslant \mu I_N\otimes P_1BB^{\mathrm{T}}P_1 \tag{31}$$

Since $c < 0$, multiplying Formula (31) by $2c$ reverses the inequality

$$\begin{aligned}2c\bar{\delta}(t)^{\mathrm{T}}(\Lambda\otimes P_1BB^{\mathrm{T}}P_1)\bar{\delta}(t) \leqslant \\ 2c\mu\bar{\delta}(t)^{\mathrm{T}}(I_N\otimes P_1BB^{\mathrm{T}}P_1)\bar{\delta}(t)\end{aligned} \tag{32}$$

Define $\tilde{c} = 2c\mu < 0$. Substituting Formula (32) into Eq. (30) gives

$$\dot{V}(t) \leqslant \bar{\delta}(t)^{\mathrm{T}}(\Pi\otimes(A^{\mathrm{T}}P_1+P_1A+\tilde{c}P_1BB^{\mathrm{T}}P_1))\bar{\delta}(t) \tag{33}$$

To further bound the term $\tilde{c}P_1BB^{\mathrm{T}}P_1$, Lemma 2 guarantees that for any $\alpha > 0$ there are $\tau > 0$ and $P_1 > 0$ such that

$$A^{\mathrm{T}}P_1+P_1A-\tau P_1BB^{\mathrm{T}}P_1 < -\alpha P_1 \tag{34}$$

Choose τ sufficiently large such that $\tau \geqslant -\tilde{c}$. Then, we have

$$\begin{aligned}A^{\mathrm{T}}P_1+P_1A+\tilde{c}P_1BB^{\mathrm{T}}P_1 \leqslant \\ A^{\mathrm{T}}P_1+P_1A-\tau P_1BB^{\mathrm{T}}P_1\end{aligned} \tag{35}$$

Combining Formulas (34) and (35) yields

$$A^{\mathrm{T}}P_1+P_1A+\tilde{c}P_1BB^{\mathrm{T}}P_1 < -\alpha P_1 \tag{36}$$

Since $\Pi > 0$, Formula (36) implies

$$\Pi\otimes(A^{\mathrm{T}}P_1+P_1A+\tilde{c}P_1BB^{\mathrm{T}}P_1) < -\alpha\Pi\otimes P_1 \tag{37}$$

Substituting Formula (37) into Formula (33) yields

$$\dot{V}(t) \leqslant -\alpha\bar{\delta}(t)^{\mathrm{T}}(\Pi\otimes P_1)\bar{\delta}(t) = -\alpha V(t) \tag{38}$$

Thus $\dot{V}(t) \leqslant -\alpha V(t)$ with $\alpha > 0$. Solving this differential inequality gives $V(t) \leqslant \mathrm{e}^{-\alpha t}V(0)$, so $V(t) \to 0$ exponentially as $t \to \infty$. Consequently $\bar{\delta}(t) \to 0$. Because the transformation $\bar{\delta}(t) = (\mathcal{D}\otimes I_n)\delta(t)$ is invertible, $\delta(t) \to 0$, meaning that for each $i = 1,2,\ldots,N$, $\lim_{t\to\infty}(x_i(t)/\omega_i - d_ix_0(t)/\omega_0) = 0$. Hence, the bipartite-scaled consensus is achieved. The proof is completed. ■

Remark 3 Formula (20) is a standard LMI in the variable $P = P^{\mathrm{T}} > 0$ for prescribed scalars $\alpha \geqslant 0$ and $\tau > 0$. It can be solved efficiently using solvers such as the MATLAB LMI Toolbox. The solution yields P, from which $\Gamma = B^{\mathrm{T}}P$ is obtained. The dimension of this LMI depends only on the agent dynamics (A, B) and is independent of the agent number N. Therefore, the computational complexity and the feasibility region do not scale with N. The graph-dependent condition on the coupling strength c is separate and does not affect the LMI's conservatism, which consequently remains bounded as N increases.

Remark 4 The distributed state feedback controller Eq. (7) is designed under the ideal assumption of no input saturation. In this ideal setting, the closed-loop error system in Eq. (15) is linear and exponentially stable, guaranteeing global convergence for any finite initial state deviations. When actuators (e.g., motors with saturation limits) are subject to saturation, the system becomes nonlinear and global exponential stability is no longer automatically assured. Nevertheless, a region of attraction exists because of the linear stability of the unsaturated dynamics and the system remains stable for initial states within this region. Moreover, relaxing the no-saturation assumption via anti-windup compensation or low-gain feedback techniques is a critical step toward practical hardware implementation.

B. Bipartite-Scaled Consensus Analysis Based on Output Feedback Controller under Fixed Topologies

Direct measurement of all states is unavailable. An observer-based output feedback scheme is then adopted. The neighborhood state estimation error of each follower is defined as

$$\sigma_i(t) = \sum_{j\in\mathcal{N}_i} |a_{ij}|\left(\frac{\hat{x}_i(t)}{\omega_i} - \operatorname{sgn}(a_{ij})\frac{\hat{x}_j(t)}{\omega_j}\right) + g_i\left(\frac{\hat{x}_i(t)}{\omega_i} - d_i\frac{x_0(t)}{\omega_0}\right) \tag{39}$$

Based on Eq. (39), the distributed output feedback controller is designed as

$$u_i(t) = c\varGamma\sigma_i(t) \tag{40}$$

The global state vector and estimated state vector are

$$x(t) = (x_1^{\mathrm{T}}(t), x_2^{\mathrm{T}}(t), \ldots, x_N^{\mathrm{T}}(t))^{\mathrm{T}},\quad \hat{x}(t) = (\hat{x}_1^{\mathrm{T}}(t), \hat{x}_2^{\mathrm{T}}(t), \ldots, \hat{x}_N^{\mathrm{T}}(t))^{\mathrm{T}} \tag{41}$$

From Eq. (2), the global closed-loop dynamics are

$$\dot{x}(t) = (I_N\otimes A)x(t) + c((L+G)\varOmega^{-1}\otimes B\varGamma)\hat{x}(t) - c(G\mathcal{D}\omega_0^{-1}\otimes B\varGamma)\bar{x}_0(t) \tag{42}$$

where $\bar{x}_0(t) = 1_N\otimes x_0(t)$.

To analyze the observer error dynamics, the neighborhood output error function is defined as

$$\zeta_i(t) = \sum_{j\in\mathcal{N}_i} |a_{ij}|(\tilde{y}_i(t) - \operatorname{sgn}(a_{ij})\tilde{y}_j(t)) + g_i(\tilde{y}_i(t) - \tilde{y}_0(t)) \tag{43}$$

where $\tilde{y}_i(t) = C\hat{x}_i(t) + Du_i(t) - y_i(t)$ is the output estimation error. Since the leader's state is perfectly known, $\hat{x}_0(t) = x_0(t)$ and $\tilde{y}_0(t) = 0$. Let $\tilde{x}(t) = x(t) - \hat{x}(t)$. Then $\tilde{y}_i(t) = C\tilde{x}_i(t)$. Equation (43) then becomes

$$\zeta_i(t) = C\Big(\sum_{j\in\mathcal{N}_i}|a_{ij}| + g_i\Big)\tilde{x}_i(t) - \sum_{j\in\mathcal{N}_i} a_{ij}C\tilde{x}_j(t) \tag{44}$$

which can be expressed compactly as

$$\zeta(t) = ((L+G)\otimes C)\tilde{x}(t) \tag{45}$$

where $\zeta(t) = (\zeta_1^{\mathrm{T}}(t), \zeta_2^{\mathrm{T}}(t), \ldots, \zeta_N^{\mathrm{T}}(t))^{\mathrm{T}}$ and $\tilde{x}(t) = (\tilde{x}_1^{\mathrm{T}}(t), \tilde{x}_2^{\mathrm{T}}(t), \ldots, \tilde{x}_N^{\mathrm{T}}(t))^{\mathrm{T}}$ are the stacked vectors.

The observer for each follower is then designed as

$$\dot{\hat{x}}_i(t) = A\hat{x}_i(t) + Bu_i(t) - cKQ\zeta_i(t) \tag{46}$$

where c is the coupling strength. $K\in\mathbb{R}^{n\times r}$ and $Q\in\mathbb{R}^{r\times r}$ are observer gain matrices to be designed.

From Eqs. (45) and (46), the global observer dynamics are

$$\dot{\hat{x}}(t) = (I_N\otimes A + c(L+G)\varOmega^{-1}\otimes B\varGamma)\hat{x}(t) - c(G\mathcal{D}\omega_0^{-1}\otimes B\varGamma)\bar{x}_0(t) - c((L+G)\otimes KQC)\tilde{x}(t) \tag{47}$$

Define the global state estimation error as $\tilde{x}(t) = x(t) - \hat{x}(t)$. Using Eqs. (42) and (47), the dynamics of $\tilde{x}(t)$ are derived as

$$\dot{\tilde{x}}(t) = \dot{x}(t) - \dot{\hat{x}}(t) = (I_N\otimes A)(x(t) - \hat{x}(t)) + c((L+G)\otimes KQC)\tilde{x}(t) = A_0\tilde{x}(t) \tag{48}$$

where

$$A_0 = I_N\otimes A + c(L+G)\otimes KQC \tag{49}$$

Define the bipartite-scaled tracking error of the i-th follower based on the estimated state as

$$\hat{\delta}_i(t) = \frac{\hat{x}_i(t)}{\omega_i} - d_i\frac{x_0(t)}{\omega_0},\quad i = 1, 2, \ldots, N \tag{50}$$

which is the estimated counterpart of $\delta_i(t)$ in Eq. (4). From Eq. (39), the neighborhood state estimation error $\sigma_i(t)$ is expressed as

$$\sigma_i(t) = \sum_{j\in\mathcal{N}_i}|a_{ij}|(\hat{\delta}_i(t) - d_id_j\hat{\delta}_j(t)) + g_i\hat{\delta}_i(t) \tag{51}$$

Its global form is

$$\sigma(t) = (L+G)\hat{\delta}(t) \tag{52}$$

with $\sigma(t) = (\sigma_1^{\mathrm{T}}(t), \sigma_2^{\mathrm{T}}(t), \ldots, \sigma_N^{\mathrm{T}}(t))^{\mathrm{T}}$ and $\hat{\delta}(t) = (\hat{\delta}_1^{\mathrm{T}}(t), \hat{\delta}_2^{\mathrm{T}}(t), \ldots, \hat{\delta}_N^{\mathrm{T}}(t))^{\mathrm{T}}$.

Using Eq. (52), the global closed-loop dynamics in Eq. (42) can be rewritten as

$$\dot{x}(t) = (I_N\otimes A)x(t) + c((L+G)\otimes B\varGamma)\hat{\delta}(t) \tag{53}$$

Left-multiplying both sides of Eq. (53) by $(\varOmega^{-1}\otimes I_n)$ and using Kronecker product properties yields

$$(\varOmega^{-1}\otimes I_n)\dot{x}(t) = (I_N\otimes A)(\varOmega^{-1}\otimes I_n)x(t) + c(\varOmega^{-1}(L+G)\otimes B\varGamma)\hat{\delta}(t) \tag{54}$$

The global bipartite-scaled tracking error vector $\delta(t)$ is

$$\delta(t) = (\varOmega^{-1}\otimes I_n)x(t) - \left(D1_N\otimes\frac{x_0(t)}{\omega_0}\right) \tag{55}$$

Substituting Eq. (55) into Eq. (54) gives

$$(\varOmega^{-1}\otimes I_n)\dot{x}(t) = (I_N\otimes A)\left(\delta(t) + \left(D1_N\otimes\frac{x_0(t)}{\omega_0}\right)\right) + c(\varOmega^{-1}(L+G)\otimes B\varGamma)\hat{\delta}(t) \tag{56}$$

Then, from Eqs. (55) and (56), one obtains

$$\begin{aligned}\dot{\delta}(t) &= (\varOmega^{-1}\otimes I_n)\dot{x}(t) - \left(D1_N\otimes\frac{Ax_0(t)}{\omega_0}\right) = \\ &(I_N\otimes A)\left(\delta(t) + \left(D1_N\otimes\frac{x_0(t)}{\omega_0}\right)\right) + \\ &c(\varOmega^{-1}(L+G)\otimes B\varGamma)\hat{\delta}(t) - \left(D1_N\otimes\frac{Ax_0(t)}{\omega_0}\right) = \\ &(I_N\otimes A)\delta(t) + c(\varOmega^{-1}(L+G)\otimes B\varGamma)\hat{\delta}(t)\end{aligned} \tag{57}$$

The relationship between $\hat{\delta}(t)$ and $\delta(t)$ is derived from Eq. (50) and the definition of $\tilde{x}(t)$.

$$\hat{\delta}_i(t) = \delta_i(t) - \frac{\tilde{x}_i(t)}{\omega_i} \Longrightarrow \hat{\delta}(t) = \delta(t) - (\varOmega^{-1}\otimes I_n)\tilde{x}(t) \tag{58}$$

Substituting Eq. (58) into Eq. (57) yields

$$\dot{\delta}(t) = (I_N\otimes A + c\varOmega^{-1}(L+G)\otimes B\varGamma)\delta(t) - c(\varOmega^{-1}(L+G)\otimes B\varGamma)(\varOmega^{-1}\otimes I_n)\tilde{x}(t) \tag{59}$$

Thus, the difference between $\hat{\delta}(t)$ and $\delta(t)$ arises from the state estimation error $\tilde{x}(t)$.

For notational convenience, define

$$B_0 = -c(\varOmega^{-1}(L+G)\otimes B\varGamma)(\varOmega^{-1}\otimes I_n) \tag{60}$$

Then, the closed-loop error dynamics become

$$\dot{\delta}(t) = A_c\delta(t) + B_0\tilde{x}(t) \tag{61}$$

where A_c is defined in Eq. (11). The overall output feedback system can be written in matrix form as

$$\begin{pmatrix} \dot{\delta}(t) \\ \dot{\tilde{x}}(t) \end{pmatrix} = \begin{pmatrix} A_c & B_0 \\ 0 & A_0 \end{pmatrix} \begin{pmatrix} \delta(t) \\ \tilde{x}(t) \end{pmatrix} \tag{62}$$

This cascaded structure shows that the stability of the closed-loop system depends on A_c and A_0. Lemma 3 provides sufficient conditions for A_0 to be Hurwitz.

Lemma 3 If the matrix pair (A, C) is detectable, there is a positive definite matrix $P_2 = P_2^{\mathrm{T}} > 0$ such that

$$A^{\mathrm{T}} P_2 + P_2 A + C^{\mathrm{T}} Q^{\mathrm{T}} Q C < 0 \tag{63}$$

where $Q \in \mathbb{R}^{r \times r}$ is a weighting matrix ensuring dimensional compatibility.

Proof Since (A, C) is detectable, there is a gain matrix K such that $A + 1/2KQC$ is Hurwitz. By the Lyapunov stability theorem, there is $P_2 = P_2^{\mathrm{T}} > 0$ satisfying

$$\begin{aligned} &\left(A + \frac{1}{2}KQC\right)^{\mathrm{T}} P_2 + P_2 \left(A + \frac{1}{2}KQC\right) = \\ &A^{\mathrm{T}} P_2 + P_2 A + \frac{1}{2} C^{\mathrm{T}} Q^{\mathrm{T}} K^{\mathrm{T}} P_2 + \frac{1}{2} P_2 K Q C < 0 \end{aligned} \tag{64}$$

Now set $K = P_2^{-1} C^{\mathrm{T}} Q^{\mathrm{T}}$. Then $P_2 K = C^{\mathrm{T}} Q^{\mathrm{T}}$ and $K^{\mathrm{T}} P_2 = QC$. Substituting into Formula (64) yields

$$\begin{aligned} &\left(A + \frac{1}{2}KQC\right)^{\mathrm{T}} P_2 + P_2 \left(A + \frac{1}{2}KQC\right) = \\ &A^{\mathrm{T}} P_2 + P_2 A + \frac{1}{2} C^{\mathrm{T}} Q^{\mathrm{T}} K^{\mathrm{T}} P_2 + \frac{1}{2} P_2 K Q C = \\ &A^{\mathrm{T}} P_2 + P_2 A + \frac{1}{2} C^{\mathrm{T}} Q^{\mathrm{T}} Q C + \frac{1}{2} C^{\mathrm{T}} Q^{\mathrm{T}} Q C = \\ &A^{\mathrm{T}} P_2 + P_2 A + C^{\mathrm{T}} Q^{\mathrm{T}} Q C < 0 \end{aligned} \tag{65}$$

Thus the desired inequality is obtained. ■

The main result under the output feedback control protocol is stated as follows.

Theorem 2 Consider the leader-follower MAS in Eqs. (2) and (3), whose interaction topology is a structurally balanced digraph containing a spanning tree with the leader as root. Given any positive scaling gain $\omega_i > 0$, Assumption 1 guarantees that the distributed output feedback law in Eq. (40) combined with observer in Eq. (46) yields bipartite-scaled consensus, provided that the subsequent conditions are satisfied.

(1) The coupling strength satisfies $c \leqslant -1/\lambda_{\max}((L+G) + (L+G)^{\mathrm{T}})$ and the feedback gain $\Gamma = B^{\mathrm{T}} P_1$ is designed as in Theorem 1.

(2) The observer gain matrix is designed as $K = P_2^{-1} C^{\mathrm{T}} Q^{\mathrm{T}}$ with $P_2 = P_2^{\mathrm{T}} > 0$ satisfying Formula (63) in Lemma 3.

Proof First, the stability of the observer error system is established. From Remark 1, there is a positive diagonal matrix Π such that $\Pi((L+G) + (L+G)^{\mathrm{T}})\Pi > 0$. Because $(L+G) + (L+G)^{\mathrm{T}}$ is positive definite under the spanning tree condition, one may simply take $\Pi = I_N$. Define the symmetric matrix

$$\Phi = \frac{1}{2}((L+G) + (L+G)^{\mathrm{T}}) > 0 \tag{66}$$

and denote $\nu = \lambda_{\min}(\Phi) > 0$. Consider the Lyapunov function

$$V_2(t) = \tilde{x}(t)^{\mathrm{T}} (I_N \otimes P_2) \tilde{x}(t) \tag{67}$$

with P_2 from Lemma 3. Differentiating $V_2(t)$ along the observer error dynamics yields

$$\begin{aligned} \dot{V}_2(t) = \tilde{x}(t)^{\mathrm{T}} (I_N \otimes (A^{\mathrm{T}} P_2 + P_2 A)) \tilde{x}(t) + \\ 2c \tilde{x}(t)^{\mathrm{T}} (\Phi \otimes C^{\mathrm{T}} Q^{\mathrm{T}} Q C) \tilde{x}(t) \end{aligned} \tag{68}$$

Because $\Phi \geqslant \nu I_N$ and $c < 0$, the second term satisfies

$$\begin{aligned} 2c \tilde{x}(t)^{\mathrm{T}} (\Phi \otimes C^{\mathrm{T}} Q^{\mathrm{T}} Q C) \tilde{x}(t) \leqslant \\ 2c\nu \tilde{x}(t)^{\mathrm{T}} (I_N \otimes C^{\mathrm{T}} Q^{\mathrm{T}} Q C) \tilde{x}(t) \end{aligned} \tag{69}$$

To ensure $\dot{V}_2(t) < 0$, it suffices to have

$$A^{\mathrm{T}} P_2 + P_2 A + 2c\nu C^{\mathrm{T}} Q^{\mathrm{T}} Q C < 0 \tag{70}$$

By Lemma 3, this holds if $2c\nu \leqslant -1$, i.e., $c \leqslant -1/(2\nu)$. Since $\lambda_{\max}((L+G) + (L+G)^{\mathrm{T}}) = 2\nu$, the condition is exactly $c \leqslant -1/\lambda_{\max}((L+G) + (L+G)^{\mathrm{T}})$. Under this choice, $\dot{V}_2(t) < 0$, implying $\tilde{x}(t) \to 0$ exponentially.

Now consider the bipartite-scaled tracking error. From Eq. (62), the error dynamics satisfy

$$\dot{\delta}(t) = A_c \delta(t) + B_0 \tilde{x}(t), \quad \dot{\tilde{x}}(t) = A_0 \tilde{x}(t) \tag{71}$$

with being A_0 Hurwitz as established above. It remains to prove that A_c is Hurwitz. Recall $A_c = I_N \otimes A + c\Omega^{-1}(L+G) \otimes B\Gamma$. Let $\mathcal{D}$ be the signature matrix from Lemma 1. Using $\mathcal{D}^2 = I_N$ and $\mathcal{D}(L+G)\mathcal{D} = \bar{L}$, one obtains the similarity relation as

$$\mathcal{D}(\Omega^{-1}(L+G))\mathcal{D} = \Omega^{-1} \bar{L} \tag{72}$$

Hence $\Omega^{-1}(L+G)$ is similar to $\Omega^{-1}\bar{L}$ and their eigenvalues coincide with those of $\bar{L}\Omega^{-1}$. Theorem 1 ensures that under the conditions $c < 0$ and $\Gamma = B^{\mathrm{T}} P_1$, the matrix $I_N \otimes A + c\bar{L}\Omega^{-1} \otimes B\Gamma$ is Hurwitz. The given coupling strength satisfies $c \leqslant -1/\lambda_{\max}((L+G) + (L+G)^{\mathrm{T}})$, which implies $c < 0$. Consequently, A_c is similar to a Hurwitz matrix and therefore also Hurwitz.

Since both A_c and A_0 are Hurwitz, the cascaded system in Eq. (62) is asymptotically stable. Consequently, $\delta(t) \to 0$, i.e., $\lim_{t \to \infty} \delta_i(t) = 0$ for all $i = 1, 2, \ldots, N$. This completes the proof. ■

Remark 5 Formula (63) is an LMI in the variable $P_2 = P_2^{\mathrm{T}} > 0$ for a prescribed matrix Q. It can be solved using standard LMI solvers, yielding P_2, from which the observer gain is constructed as $K = P_2^{-1} C^{\mathrm{T}} Q^{\mathrm{T}}$. Unlike the LMI in Lemma 2, which involves an additional scalar τ, the LMI here contains only the matrix variable P_2 and a fixed weighting matrix Q. Both LMIs share the property that their dimensions depend solely on the agent dynamics (A, B) or (A, C) and are independent of the number of agents N. Consequently, the computational complexity and the feasibility region do not scale with N. The graph-dependent condition on c in Theorem 2 is a separate scalar inequality and does not introduce extra conservatism into the LMI. Thus, the design remains scalable to large-scale MASs.

Remark 6 Unlike the existing leader-follower scaled consensus results [12–16] that assume purely cooperative networks, the proposed framework simultaneously handles cooperative-competitive interactions and prescribed asymmetric scaling. Neither Laplacian symmetry nor the real-part eigenvalue condition is required, so the method applies to directed signed graphs. Furthermore, bipartite antagonism encoded by the signature matrix $\mathcal{D}$ and flexible scaling factors ω_i and ω_0 are integrated into a unified design, relaxing the equal-magnitude constraint of conventional bipartite consensus and extending scaled consensus to signed topologies.

C. Bipartite-Scaled Consensus under Switching Topologies

In practical MASs, the communication topology may change over time because of link failures, packet dropouts, and limited communication ranges. To accommodate such scenarios, we consider switching topologies. Let $\sigma(t): [0,\infty) \to \mathcal{P}$ be a piecewise constant switching signal. The neighbor set $\mathcal{N}_i(t)$ and pinning gains $g_i(t)$ become time-varying accordingly. In this paper, we assume that $\sigma(t)$ is non-Zeno, i.e., only finitely many switches occur in any finite time interval. This is a standard assumption in switched system analysis to ensure well-defined trajectories.

Assumption 2 For the non-Zeno switching signal $\sigma(t)$, every directed signed graph $\mathcal{G}_{\sigma(t)}$ is structurally balanced and the union (or convex combination) formed by all possible topologies includes a directed spanning tree rooted at the leader.

Under switching topologies, the distributed state feedback controller for each agent is designed as

$$\begin{aligned} u_i(t) = c\Gamma \sum_{j\in\mathcal{N}_i(t)} |a_{ij}(t)| \left(\frac{x_i(t)}{\omega_i} - \operatorname{sgn}(a_{ij}(t)) \frac{x_j(t)}{\omega_j} \right) + \\ g_i(t) \left(\frac{x_i(t)}{\omega_i} - d_i(t) \frac{x_0(t)}{\omega_0} \right) \end{aligned} \tag{73}$$

where $c < 0$ and Γ are the coupling strength and feedback gain as in the fixed topology case.

Substituting Eq. (73) into Eq. (2) and using the definition of Eq. (4), after similar algebraic manipulations as in the fixed topology case, the global error dynamics under switching topologies can be obtained as

$$\dot{\delta}(t) = (I_N \otimes A + c\bar{L}_{\sigma(t)} \Omega^{-1} \otimes B\Gamma)\delta(t) \tag{74}$$

where $\bar{L}_{\sigma(t)} = \mathcal{D}(L_{\sigma(t)} + G_{\sigma(t)})\mathcal{D}$ is positive definite for each mode under the spanning tree condition.

Theorem 3 Consider the leader-follower MAS described by Eqs. (2) and (3) under switching directed signed graphs satisfying Assumption 2. For any prescribed scaling factor $\omega_i > 0$, the bipartite-scaled consensus is achieved by the distributed state feedback controller in Eq. (73) under Assumption 1, if the following conditions hold.

(1) The coupling strength satisfies $c < 0$.

(2) The feedback gain matrix is designed as $\Gamma = B^{\mathrm{T}} P_3$, where $P_3 = P_3^{\mathrm{T}} > 0$ is a matrix solution of Formula (20) in Lemma 2.

Proof For each switching mode $\sigma(t)$, from Remark 1 there is a positive diagonal matrix Π such that $\Pi(\bar{L}_{\sigma(t)} + \bar{L}_{\sigma(t)}^{\mathrm{T}})\Pi > 0$. Similar to the fixed topology case, we take $\Pi = \Omega^{-1}$, which satisfies the inequality. Notably, this Lyapunov function candidate is common to all switching modes because Π and P_3 are mode-independent. Define the following symmetric matrix

$$\phi = \frac{1}{2}(\Pi \bar{L}_{\sigma(t)} \Omega^{-1} + \Omega^{-1} \bar{L}_{\sigma(t)}^{\mathrm{T}} \Pi) \tag{75}$$

and let $\gamma = \lambda_{\min}(\phi) > 0$.

Consider the Lyapunov function

$$V(t) = \delta(t)^{\mathrm{T}} (\Pi \otimes P_3) \delta(t) \tag{76}$$

Differentiating $V(t)$ along the trajectory of Eq. (74) and substituting $\Gamma = B^{\mathrm{T}} P_3$, followed by simplification, yields

$$\begin{aligned} \dot{V}(t) = \delta(t)^{\mathrm{T}} (\Pi \otimes (A^{\mathrm{T}} P_3 + P_3 A)) \delta(t) + \\ 2c\delta(t)^{\mathrm{T}} (\phi \otimes P_3 B B^{\mathrm{T}} P_3) \delta(t) \end{aligned} \tag{77}$$

Since $\phi \geqslant \gamma I_N$ and $c < 0$, the second term satisfies

$$\begin{aligned} 2c\delta(t)^{\mathrm{T}} (\phi \otimes P_3 B B^{\mathrm{T}} P_3) \delta(t) \leqslant \\ 2c\gamma \delta(t)^{\mathrm{T}} (I_N \otimes P_3 B B^{\mathrm{T}} P_3) \delta(t) \end{aligned} \tag{78}$$

Define $\bar{c} = 2c\gamma < 0$. Then, we have

$$\dot{V}(t) \leqslant \delta(t)^{\mathrm{T}} (A^{\mathrm{T}} P_3 + P_3 A + \bar{c} P_3 B B^{\mathrm{T}} P_3) \delta(t) \tag{79}$$

By Lemma 2, for any $\alpha > 0$ there are $\tau > 0$ and $P_3 > 0$ such that

$$A^{\mathrm{T}} P_3 + P_3 A - \tau P_3 B B^{\mathrm{T}} P_3 < -\alpha P_3 \tag{80}$$

Choosing $\tau \geqslant -\bar{c}$ gives

$$\begin{aligned} A^{\mathrm{T}} P_3 + P_3 A + \bar{c} P_3 B B^{\mathrm{T}} P_3 \leqslant \\ A^{\mathrm{T}} P_3 + P_3 A - \tau P_3 B B^{\mathrm{T}} P_3 < -\alpha P_3 \end{aligned} \tag{81}$$

Since $\Pi > 0$, the Kronecker product preserves Formula (81), leading to

$$\dot{V}(t) \leqslant -\alpha \delta(t)^{\mathrm{T}} (\Pi \otimes P_3) \delta(t) = -\alpha V(t) \tag{82}$$

Thus $\dot{V}(t) \leqslant -\alpha V(t)$ with $\alpha > 0$, implying $V(t) \to 0$ exponentially as $t \to \infty$. Consequently $\delta(t) \to 0$ and bipartite-scaled consensus is achieved under switching topologies. Therefore, the convergence holds for arbitrary non-Zeno switching signals without requiring any dwell-time or average dwell-time (ADT) constraints. ■

Remark 7 In this paper, we adopt a common Lyapunov function approach to handle switching topologies. This method requires neither a minimum dwell-time nor an average dwell-time condition. Exponential stability is guaranteed for any non-Zeno switching signal, including arbitrarily fast switching, as long as each mode satisfies structural balance and contains a directed spanning tree rooted at the leader. Therefore, no upper bound on the switching frequency is needed and the convergence result holds uniformly for all admissible switching signals.

D. Bipartite-Scaled Consensus Analysis Based on Output Feedback Controller under Switching Topologies

In practical MASs, when the communication topology is time-varying and the full state information is not directly measurable, the observer-based output feedback controller must be adapted to switching topologies. To address this scenario, we extend the observer-based control scheme to switching topologies.

Let $\sigma(t): [0,\infty) \to \mathcal{P}$ be a piecewise constant switching signal, where $\mathcal{P}$ denotes the set of all possible directed signed graphs. Under directed switching topologies, the distributed observer-based output feedback controller for each agent is designed as

$$
\begin{aligned}
u_i(t) = c\Gamma \sum_{j\in\mathcal{N}_i(t)} |a_{ij}(t)| \left(\frac{\hat{x}_i(t)}{\omega_i} - \mathrm{sgn}(a_{ij}(t)) \frac{\hat{x}_j(t)}{\omega_j} \right) + \\
g_i(t) \left(\frac{\hat{x}_i(t)}{\omega_i} - d_i(t) \frac{x_0(t)}{\omega_0} \right)
\end{aligned} \tag{83}
$$

where $c < 0$ is the coupling strength, Γ is the feedback gain matrix, and $\hat{x}_i(t)$ denotes the estimated state of the i-th follower. The observer dynamics under switching topologies are given by

$$
\dot{\hat{x}}_i(t) = A\hat{x}_i(t) + Bu_i(t) - cKQ\zeta_i(t) \tag{84}
$$

where $\zeta_i(t)$ is the neighborhood output error defined in Eq. (47) and K and Q are observer gain matrices.

Theorem 4 Consider the leader-follower MAS described by Eqs. (2) and (3) under switching directed signed graphs satisfying Assumption 2. For any prescribed scaling factors $\omega_i > 0$, the bipartite-scaled consensus is achieved by the distributed observer-based output feedback controller in Eq. (83) under Assumption 1, if the following conditions hold.

(1) The coupling strength satisfies $c \leqslant -1/\lambda_{\max}((L+G)_{\sigma(t)} + (L+G)^{\mathrm{T}}_{\sigma(t)})$ for each switching mode and the feedback gain matrix is designed as $\Gamma = B^{\mathrm{T}}P_3$, where $P_3 = P_3^{\mathrm{T}} > 0$ satisfies Formula (20) in Lemma 2.

(2) The observer gain matrix is designed as $K = P_4^{-1}C^{\mathrm{T}}Q^{\mathrm{T}}$ with $P_4 = P_4^{\mathrm{T}} > 0$ satisfying Formula (63) in Lemma 3.

Proof The proof follows a similar line as in Theorem 2, combining the common Lyapunov function approach for switching topologies with the observer error dynamics. Because of the space limitations, the detailed proof is omitted here. ■

IV. SIMULATIONS

Example 1 For the fixed topology case, we consider a directed signed graph that is structurally balanced and contains a directed spanning tree. Followers are partitioned into two antagonistic subgroups $\mathcal{V}_1 = \{1,2,3\}$ and $\mathcal{V}_2 = \{4,5\}$ based on the signed graph structure as depicted in Fig. 1.

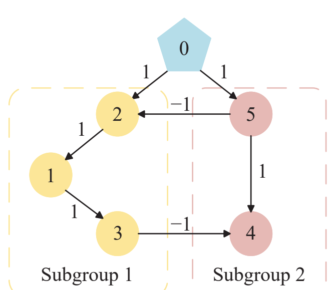

Fig. 1 Fixed communication topology of the MAS.

The corresponding Laplacian matrix L and signature matrix D are given as

$$
L = \begin{pmatrix} 1 & -1 & 0 & 0 & 0 \\ 0 & 1 & 0 & 0 & 1 \\ -1 & 0 & 2 & 1 & 0 \\ 0 & 0 & 0 & 1 & -1 \\ 0 & 0 & 0 & 0 & 1 \end{pmatrix},
$$

$$
D = \begin{pmatrix} -1 & 0 & 0 & 0 & 0 \\ 0 & -1 & 0 & 0 & 0 \\ 0 & 0 & -1 & 0 & 0 \\ 0 & 0 & 0 & 1 & 0 \\ 0 & 0 & 0 & 0 & 1 \end{pmatrix}.
$$

The system matrices in Eqs. (2) and (3) are specified as

$$
A = \begin{pmatrix} 0 & 1 \\ -1 & 0 \end{pmatrix},\quad B = \begin{pmatrix} 0 \\ 1 \end{pmatrix},\quad C = \begin{pmatrix} 1 & 0 \end{pmatrix},\quad D = 0.
$$

The feedback gain in Eq. (7) is designed as $c = -1$ and $\Gamma = -(1,3)^{\mathrm{T}}$. The scaling factor matrix is chosen as $\Omega = \mathrm{diag}(0.1, 0.2, 0.3, 0.4, 0.5)$. The simulation results are presented in Figs. 2 and 3. As observed in Fig. 2, the leader's trajectory is sinusoidal. Under the prescribed scaling coefficients, the states of followers 1, 2, and 3 (subgroup $\mathcal{V}_1$) converge to $x_i(t) \to -\omega_i x_0(t)$, while those of followers 4 and 5 (subgroup $\mathcal{V}_2$) converge to $x_i(t) \to \omega_i x_0(t)$, where ω_i is the diagonal entry of Ω. This demonstrates that the proposed protocol achieves bipartite-scaled consensus as defined in Problem 1. From Fig. 3, the tracking errors $\delta_i(t)$ of all followers decay from their initial values and asymptotically approach zero, confirming that the designed control protocol

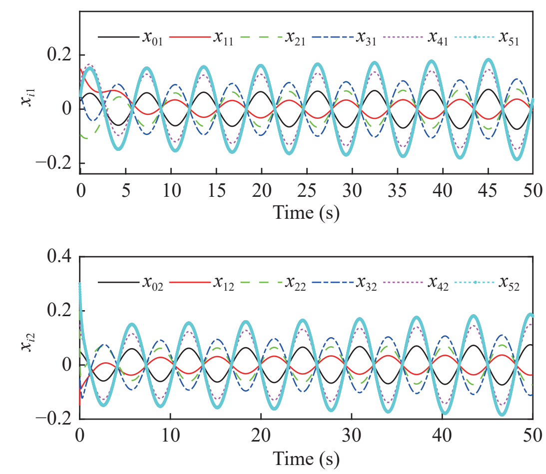

Fig. 2 Trajectories of respective agents under the fixed topologies.

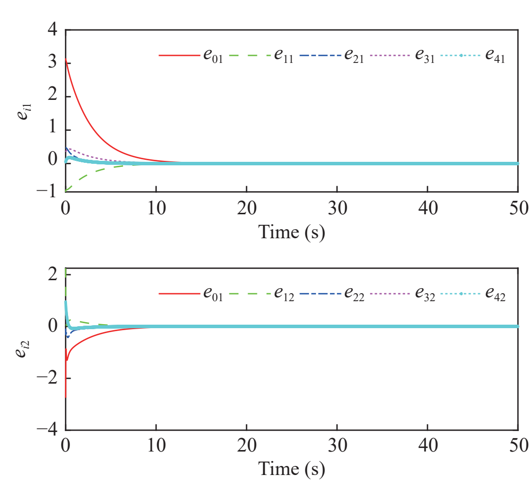

Fig. 3 Bipartite-scaled consensus errors.

effectively realizes bipartite-scaled consensus under signed graphs and verifying Theorem 1.

Example 2 To demonstrate the advantage of the proposed method, all other parameters and settings remain exactly the same as in Example 1, with only the scaling factors being adjusted. The scaling factor matrix is chosen as $\Omega = \mathrm{diag}(1,1,1,1,1)$. As shown in Fig. 4, standard bipartite consensus forces the two subgroups to converge to values with equal magnitude and opposite sign, failing to satisfy scenarios where different scaling ratios are required. In contrast, the proposed method in Example 1 successfully achieves individually prescribed scaling factors, demonstrating superior flexibility.

Example 3 To verify the applicability of the proposed method to directed graphs, the topology in Fig. 1 is changed from directed to undirected while keeping all other settings identical to Example 1. The corresponding Laplacian matrix L and signature matrix D are given as

$$L = \begin{pmatrix} 2 & -1 & -1 & 0 & 0 \\ -1 & 0 & 0 & 0 & 1 \\ -1 & 0 & 0 & 1 & 0 \\ 0 & 0 & 1 & 0 & -1 \\ 0 & 1 & 0 & -1 & 0 \end{pmatrix},$$

$$D = \begin{pmatrix} -1 & 0 & 0 & 0 & 0 \\ 0 & -1 & 0 & 0 & 0 \\ 0 & 0 & -1 & 0 & 0 \\ 0 & 0 & 0 & 1 & 0 \\ 0 & 0 & 0 & 0 & 1 \end{pmatrix}.$$

The simulation results in Fig. 5 show that bipartite-scaled consensus is still achieved. Moreover, the convergence speed under the directed graph is comparable to that under the undirected graph, confirming that the proposed method does not rely on graph symmetry and is effective for general directed signed graphs.

Example 4 To verify the effectiveness of the proposed observer-based output feedback control scheme under switching topologies, we consider a family of directed signed graphs $\{\mathcal{G}_{\sigma(t)}\}_{\sigma(t)\in\mathcal{P}}$, where $\sigma(t):[0,\infty)\to\mathcal{P}$ is a piecewise constant switching signal and $\mathcal{P}$ denotes the set of all possible directed

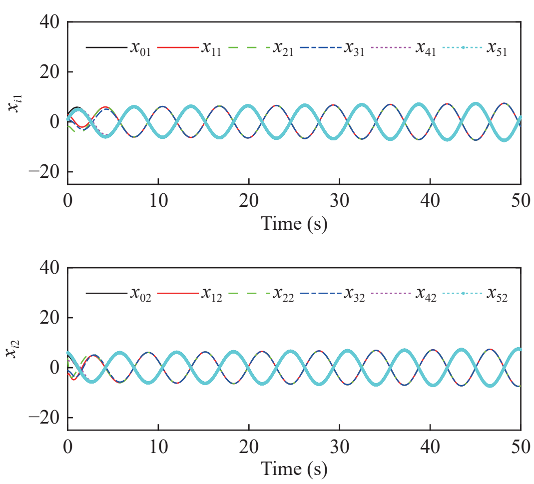

Fig. 4 Trajectories of respective agents ($\omega_i = \omega_0 = 1$).

signed graphs. The switching signal is designed such that the topology switches every 0.5 s among four structurally balanced graphs, each containing a directed spanning tree rooted at the leader. As illustrated in Fig. 6, the followers are divided into two antagonistic subgroups $\mathcal{V}_1 = \{1,2,3\}$ and $\mathcal{V}_2 = \{4,5\}$ according to the signed graph structure. The corresponding Laplacian matrix $L_{\sigma(t)}$ and signature matrix $D_{\sigma(t)}$ vary with the switching signal, but maintain the same subgroup partition.

The system matrices are the same as those in Example 1. The feedback gain is designed as $c = -1$ and $\Gamma = (-5, 5)^{\mathrm{T}}$. The observer gain parameters of distributed state observer in Eq. (84) are selected as

$$K = \begin{pmatrix} -5 & -3 \end{pmatrix}, \quad Q = \begin{pmatrix} 1.0568 & 0.0500 \\ 0.0500 & 1.0568 \end{pmatrix}.$$

The scaling factor matrix is chosen as $\Omega = \mathrm{diag}(0.15, 0.30, 0.25, 0.20, 0.35)$.

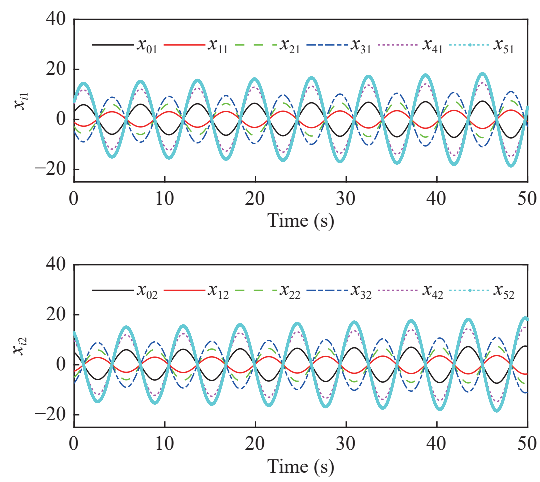

Fig. 5 Trajectories of respective agents under undirected connected topology.

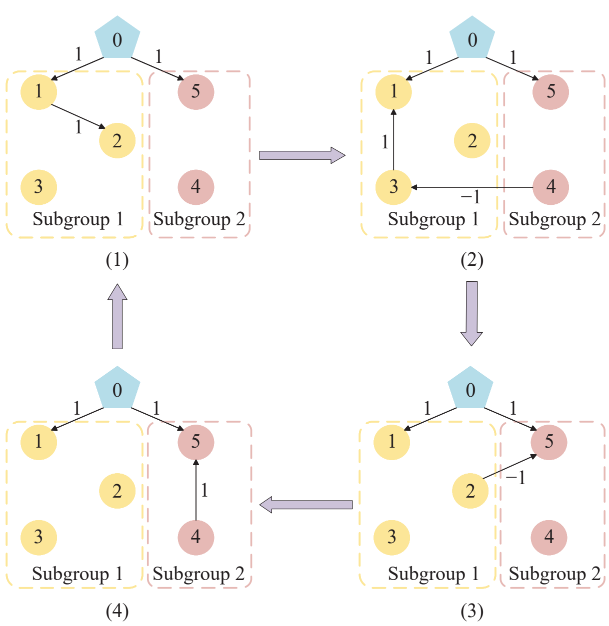

Fig. 6 Switching communication topology of the MAS.

The simulation results for the observer-based output feedback control scheme under switching topologies are presented in Figs. 7 and 8. As observed in Fig. 7, the proposed controller ensures that followers in $\mathcal{V}_1$ and $\mathcal{V}_2$ converge to the leader's scaled trajectory with opposite signs. From Fig. 8, the tracking errors $\delta_i(t)$ asymptotically approach zero despite the absence of direct state measurements and the presence of topology switching.

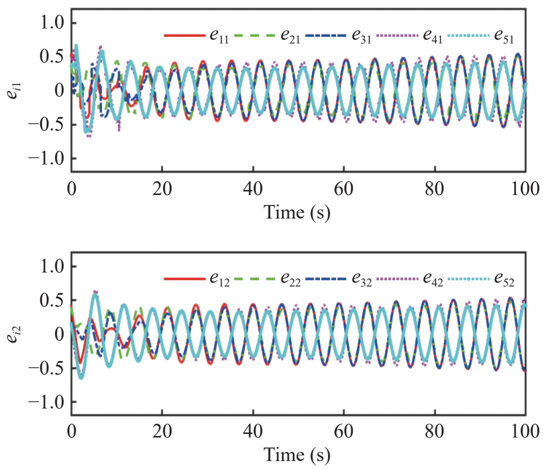

Fig. 7 Trajectories of respective agents under the switching topologies.

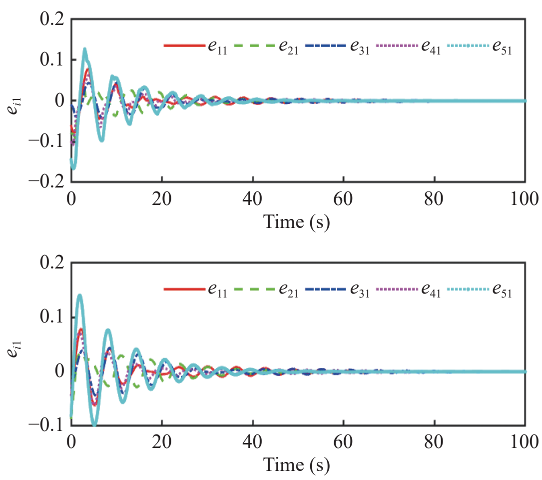

Fig. 8 Bipartite-scaled consensus errors.

V. Conclusion

This paper addresses bipartite-scaled consensus for leader-follower MASs under fixed and switching topologies with cooperative-competitive interactions. The main challenge is to achieve prescribed asymmetric scaling between two antagonistic subgroups and the leader while handling unmeasurable states and time-varying graphs. The free assignment of scaling factors allows the leader's influence on each subgroup to be adjusted independently, which is relevant for heterogeneous multi-robot systems and other practical applications. A distributed state feedback controller is developed for systems with full state measurements, and an observer-based output feedback controller is proposed for cases where states are unmeasurable. Both schemes are extended to switching topologies. The proposed framework relaxes the equal-magnitude constraint of conventional bipartite consensus and enables flexible scaling ratios. Numerical simulations verify the theoretical results. Future research includes extending to heterogeneous nonlinear MASs, actuator faults, communication delays, event-triggered mechanisms, and relaxing the no-saturation assumption via anti-windup or low-gain techniques for hardware implementation.

Acknowledgment

This work was supported by the Special Fund for Science and Technology Innovation Teams of Shanxi Province (No. 202304051001004).

References

[1] H. Yang, Y. Wang, K. Jiang, Y.-S. Ong, and Y. Song, Prescribed-time consensus tracking of multiagent systems under denial-of-service attacks with application to unmanned vehicles, *IEEE Trans. Syst., Man, Cybern.: Syst.*, 2026, 56(5), 3075–3085.

[2] J. Zhao, F. Li, S. Mukherjee, and C. Sticht, Deep reinforcement learning-based model-free on-line dynamic multi-microgrid formation to enhance resilience, *IEEE Trans. Smart Grid*, 2022, 13(4), 2557–2567.

[3] M. Hua, X. Qi, D. Chen, K. Jiang, Z. Liu, H. Sun, Q. Zhou, and H. Xu, Multi-agent reinforcement learning for connected and automated vehicles control: Recent advancements and future prospects, *IEEE Trans. Autom. Sci. Eng.*, 2025, 22, 16266–16286.

[4] X. Lu, T. Wang, Y. Zhao, and J.-F. Zhang, Consensus of multi-agent systems under binary-valued measurements: An event-triggered coordination approach, *Automatica*, 2025, 176, 112255.

[5] Z. Zuo, J. Tang, R. Ke, B. Ning, and Q.-L. Han, Fixed-time consensus control of general dynamical multiagent systems: Methodologies and applications, *IEEE Trans. Industr. Inform.*, 2026, 22(4), 2613–2626.

[6] X. Luan, N. Qing, and F. Liu, Ring-patterned control for hyperexponential consensus of multi-agent systems with increasing scales, *IEEE Trans. Autom. Control*, 2026, 1–8.

[7] L. Chen, C. Wei, and H. Duan, Multiple unmanned aerial vehicles coalition formation and control for collaborative defense mission, *IEEE Trans. Aerosp. Electron. Syst.*, 2024, 60(5), 6095–6109.

[8] C. Altafini, Consensus problems on networks with antagonistic interactions, *IEEE Trans. Autom. Control*, 2013, 58(4), 935–946.

[9] X.-F. Zhao, T. Han, B. Xiao, X.-S. Zhan, and H. Yan, Finite-time and fixed-time bipartite consensus tracking for second-order multi-agent systems via an integral sliding-mode approach, *Int. J. Control Autom. Syst.*, 2023, 21(12), 3922–3931.

[10] J. Liu, X. Ma, and H. Li, Group-bipartite consensus for heterogeneous multi-agent systems with general linear dynamics, *Asian J. Control*, 2026, 28, 1–17.

[11] W. Zhang, Q. Huang, and A. Alhudhaif, Event-triggered fixed-time bipartite consensus for nonlinear disturbed multi-agent systems with leader-follower and leaderless controller, *Inform. Sci.*, 2024, 662, 120243.

[12] Q. Wang, Scaled consensus of multi-agent systems with output saturation, *J. Franklin Inst.*, 2017, 354(14), 6190–6199.

[13] M. Li, F. Deng, and H. Ren, Scaled consensus of multi-agent systems with switching topologies and communication noises, *Nonlinear Anal. Hybrid Syst.*, 2020, 36, 100839.

[14] Y. Shang, Scaled consensus of switched multi-agent systems, *IMA J. Math. Control Inform.*, 2019, 36(2), 639–657.

[15] Y. Yang, B. Shen, and Q.-L. Han, Dynamic event-triggered scaled

consensus of multi-agent systems in reliable and unreliable networks, *IEEE Trans. Syst., Man, Cybern.: Syst.*, 2024, 54(2), 1124–1136.

[16] M. Wang, Z. Chen, Z. Yu, and H. Jiang, Event-triggered proportional consensus with input constraints in adversarial networks, *AIMS Math.*, 2025, 10(10), 23564–23589.

[17] J. Lv, C. Wang, B. Liu, Y. Kao, and Y. Jiang, Fully distributed prescribed-time consensus control of multiagent systems under fixed and switching topologies, *Inform. Sci.*, 2023, 648, 119538.

[18] C. Tian, K. Tian, J. Mei, and G. Ma, Bipartite leaderless position consensus of heterogeneous uncertain multi-agent systems under switching directed graphs, *Syst. Control Lett.*, 2023, 181, 105628.

[19] X. Yang, J. Hu, C. Tan, and X. Yi, Prediction-based scaled consensus control for heterogeneous multi-agent systems under switching topologies, *Nonlinear Dyn.*, 2024, 112(6), 4529–4550.

[20] J. Zhang, D.-W. Ding, Y. Lu, C. Deng, and Y. Ren, Distributed fault-tolerant bipartite output synchronization of discrete-time linear multiagent systems, *IEEE Trans. Cybern.*, 2023, 53(2), 1360–1373.

[21] G. Wen, Z. Duan, W. Ren, and G. Chen, Distributed consensus of multi-agent systems with general linear node dynamics and intermittent communications, *Int. J. Robust Nonlinear Control*, 2014, 24(16), 2438–2457.

Siyu Liu received the BS degree in automation from University of Jinan, Jinan, China, in 2025. She is currently pursuing the MS degree in control engineering at Taiyuan University of Science and Technology, Taiyuan, China. Her research interests include cooperative control of multi-agent systems.

Jie Zhang received the MS degree in control theory and control engineering from Yanshan University, Qinhuangdao, China, in 2018, and the PhD degree in control science and engineering from University of Science and Technology Beijing, Beijing, China, in 2022. He is currently an associate professor at School of Electronics Information Engineering, Taiyuan University of Science and Technology, Taiyuan, China. His research interests include cooperative output regulation and fault-tolerant control of multi-agent systems.

Junping Wang received the BS degree in automation from Qingdao University of Science and Technology, Qingdao, China, in 2025. He is currently pursuing the MS degree in control science and engineering at Taiyuan University of Science and Technology, Taiyuan, China. His research interests include cooperative control of multi-agent systems.

Dawei Ding received the BE degree from Ocean University of China, Qingdao, China, in 2003, and the PhD degree in control theory and engineering from Northeastern University, Shenyang, China, in 2010. He is currently a professor and associate dean at School of Automation and Electrical Engineering, University of Science and Technology Beijing, Beijing, China. He is supported by the Program for New Century Excellent Talents in University of the Ministry of Education of China. His research interests include robust control and filtering, fuzzy control, fault detection, and cyber-physical systems.